Appendix D.2

Hanford Site-Wide SSHAC Level 3 PSHA Project

April 24, 2014

Hazard Input Document (HID)
Final GMC Model

Contents

Appendix D.2 Hanford Site-Wide SSHAC Level 3 PSHA Project 1
Overview 2
Median Motions from Crustal Earthquakes 2
Median Motions from Subduction Earthquakes 5
Sigma Model for Crustal Earthquakes 7
Sigma Model for Subduction Earthquakes 8

Hanford Site-wide SSHAC Level 3 PSHA Project

April 24, 2014

Hazard Input Document (HID)
Final GMC Model

Overview

The GMC logic-tree is defined by two separate models, one for crustal earthquakes and another for subduction zone earthquakes. For both types of sources, the logic-tree defines alternative branches for the prediction of median spectral accelerations and for the associated standard deviations of the residuals (sigma). The model is fully defined at 20 oscillator periods: 0.01, 0.02, 0.03, 0.04, 0.05, 0.075, 0.10, 0.15, 0.2, 0.3, 0.4, 0.5, 0.75, 1.0, 1.5, 2.0, 3.0, 5.0, 7.5 and 10.0 seconds. All required coefficients and factors for all 20 oscillator periods are provided in Excel spreadsheets that are submitted as supplements to the HID, for ease of transfer into the hazard code.

Median Motions from Crustal Earthquakes

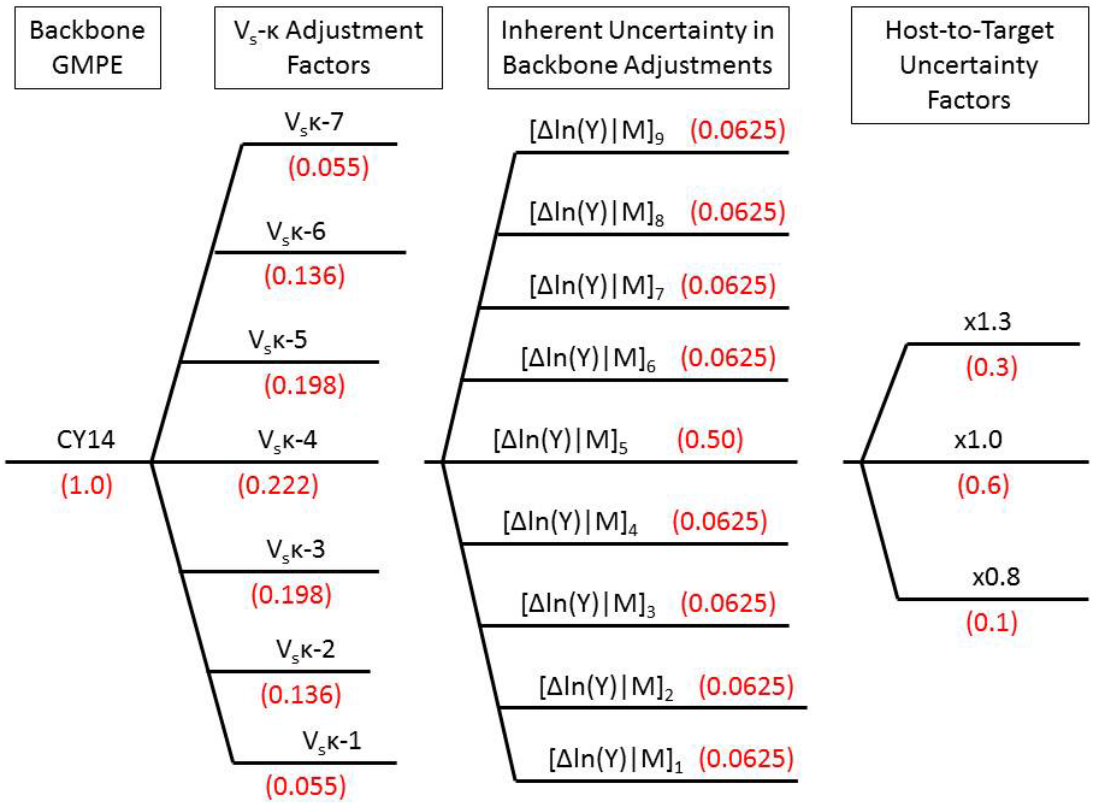

Figure GMC1. Logic-tree for median motions from crustal earthquakes.

The logic-tree for median motions from crustal earthquakes is constructed from a backbone GMPE (the 2014 model of Chiou & Youngs, hereafter CY14, as pre-published in *Earthquake Spectra*) adjusted by 7 different V_s-kappa factors. These 7 new models are then transformed to 189 (7*9*3) final median models by the application of 27 scaling factors given by the product of 9 branches for inherent uncertainty in the adjustments to the backbone model (additive in natural-log space) and another 3 for host-to-target uncertainty (multiplicative on amplitudes), as illustrated in Figure GMC1.

The CY14 model for spectral accelerations is composed of two parts, the first predicting the spectral acceleration at a reference rock site, y_{ref}, which corresponds to a V_{s30} value of 1130 m/s; this is then transformed to the target V_{s30} through application of a nonlinear site adjustment factor. The equation for predicting y_{ref} (in units of *g*) is:

$$
\begin{aligned}
\ln(\boldsymbol{y_{ref}}) = \boldsymbol{c}_1 &+ \left\{\boldsymbol{c_{1a}} + \frac{\boldsymbol{c_{1c}}}{\cosh(2.\max(\boldsymbol{M}-4.5,0))}\right\}\boldsymbol{F_{RV}} + \left\{\boldsymbol{c_{1b}} + \frac{\boldsymbol{c_{1d}}}{\cosh(2.\max(\boldsymbol{M}-4.5,0))}\right\}\boldsymbol{F_{NM}} \\
&+ \left\{\boldsymbol{c}_7 + \frac{\boldsymbol{c_{7b}}}{\cosh(2.\max(\boldsymbol{M}-4.5,0))}\right\}\Delta\boldsymbol{Z_{TOR}} + \left\{\boldsymbol{c}_{11} + \frac{\boldsymbol{c_{11b}}}{\cosh(2.\max(\boldsymbol{M}-4.5,0))}\right\}(\cos\boldsymbol{\delta})^2 \\
&+ \boldsymbol{c}_2(\boldsymbol{M}-6) + \frac{\boldsymbol{c}_2-\boldsymbol{c}_3}{\boldsymbol{c_n}}\ln(1+\boldsymbol{e}^{\boldsymbol{c_n}(\boldsymbol{c_M}-\boldsymbol{M})}) + \boldsymbol{c}_4\ln(\boldsymbol{R_{rup}} + \boldsymbol{c}_5\cosh(\boldsymbol{c}_6.\max(\boldsymbol{m}-\boldsymbol{c_{HM}},0))) \\
&+ (\boldsymbol{c_{4a}}-\boldsymbol{c}_4)\ln(\sqrt{\boldsymbol{R}_{\boldsymbol{RUP}}^2+\boldsymbol{c}_{\boldsymbol{RB}}^2}) + \left\{\boldsymbol{c}_{\gamma 1} + \frac{\boldsymbol{c}_{\gamma 2}}{\cosh(\max(\boldsymbol{M}-\boldsymbol{c}_{\gamma 3},0))}\right\}\boldsymbol{R_{RUP}} \\
&+ \boldsymbol{c}_8\max\left(1-\frac{\max(\boldsymbol{R_{RUP}}-40,0)}{30},0\right)\min\left(\frac{\max(\boldsymbol{M}-5.5,0)}{0.8},1\right)\boldsymbol{e}^{-\boldsymbol{c_{8a}}(\boldsymbol{M}-\boldsymbol{c_{8b}})^2}.\Delta\boldsymbol{DPP} \\
&+ \boldsymbol{c}_9\boldsymbol{F_{HW}}\cos(\boldsymbol{\delta})\left\{\boldsymbol{c_{9a}} + (1-\boldsymbol{c_{9a}})\tanh\left(\frac{\boldsymbol{R_x}}{\boldsymbol{c_{9b}}}\right)\right\}\left\{1-\frac{\sqrt{\boldsymbol{R}_{\boldsymbol{JB}}^2+\boldsymbol{Z}_{\boldsymbol{TOR}}^2}}{\boldsymbol{R_{RUP}}+1}\right\}
\end{aligned}
\qquad (1)
$$

The median (mean log) spectral acceleration for the target site condition is then obtained from the following expression:

$$
\begin{aligned}
\overline{\ln(y)} = \ln(y_{ref}) &+ \phi_1.\min\left[\ln\left(\frac{V_{s30}}{1130}\right),0\right] + \phi_5\left(1-e^{-\Delta Z_{1.0}/\phi_6}\right) \\
&+ \phi_2\left(e^{\phi_3(\min(V_{s30},1130)-360)} - e^{\phi_3(1130-360)}\right)\ln\left(\frac{y_{ref}+\phi_4}{\phi_4}\right)
\end{aligned}
\qquad (2)
$$

The predictor variables in these equations are as follows:

M	Moment magnitude
R_{RUP}	Closest distance to rupture plane (km)
R_{JB}	Joyner-Boore distance (km)
R_x	Perpendicular (to fault strike) distance to site from the fault line (surface projection of top of rupture), positive in the down-dip direction (km)
F_{HW}	Hanging-wall factor: 1 for $R_X \geq 0$, 0 for $R_X < 0$.
δ	Fault dip angle
Z_{TOR}	Depth to top of rupture (km)
ΔZ_{TOR}	Z_{TOR} centered on M-dependent average Z_{TOR} (*see below*)
F_{RV}	Flag for reverse/reverse-oblique faulting: 1 for 30° ≤ λ ≤ 150°, 0 otherwise
F_{NM}	Flag for normal faulting: 1 for -120° ≤ λ ≤ -60°, 0 otherwise; excludes normal-oblique faulting
V_{s30}	Time-averaged shear-wave velocity over top 30 m (m/s); this is set to 760 m/s for these calculations (assumed host value)
$Z_{1.0}$	Depth to shear-wave velocity of 1.0 km/s (m) (*see below*)
$\Delta Z_{1.0}$	$Z_{1.0}$ centered on the V_{s30}-dependent average $Z_{1.0}$ (*see below*)
ΔDPP	DPP centered on site- and earthquake-specific average DPP (*see below*)

The parameter ΔZ_{TOR} is calculated as the value of Z_{TOR} for the earthquake under consideration minus the mean value for earthquakes of magnitude **M,** $\overline{Z_{TOR}(M)}$**.** To account for the higher near-surface crustal strength of the basalts compared to typical active tectonic region crust, ΔZ_{TOR} is computed by the equation:

$$\Delta Z_{TOR} = \max[Z_{TOR}, 3] - \overline{Z_{TOR}(M)} \tag{3}$$

The value of $\overline{Z_{TOR}(M)}$ is computed from Equation (4a) for reverse and reverse-oblique faulting or from Equation (4b) for strike-slip or normal faulting:

$$\overline{Z_{TOR}(M)} = \max[2.704 - 1.266.\max(M - 5.849, 0), 0]^2 \tag{4a}$$

$$\overline{Z_{TOR}(M)} = \max[2.673 - 1.136.\max(M - 4.970, 0), 0]^2 \tag{4b}$$

For the host region (California) classification, for V_{s30} = 760 m/s, the estimated value of $Z_{1.0}$ for all locations is 27.4 m. Since this is an estimated rather than measured value (since it corresponds to an ideal host site profile), the term $\Delta Z_{1.0}$ is 0.0 for all sites.

For these hazard calculations, rupture directivity effects will not be included, hence the term ΔDPP is set to zero.

The values of the coefficients of Equations (1) and (2) for the 20 response periods are given in Excel file ***Hanford_GMC_Crustal_median_CY14_coefficients.xlsx***.

The values of the V_s-kappa adjustment factors for the 20 target oscillator periods and the five target sites are in the Excel file ***Hanford_GMC_Crustal_VsKappa factors.xlsx.***

The period-dependent adjustment factors for the inherent epistemic uncertainty in the median backbone are given by Equation (5)

$$\Delta \ln(Y) = p_1 + p_2(M-6.5) + p_3 \max(M-7,0) + \\ F_{HW}\{1+p_4\cos(\delta)\} \times \ln\left[p_5 \cosh\{p_6 \max(\ln(R_X / p_7),0)\}\right] \times \exp(p_8 R_{JB}) \times \max[0, \min(M,6.5)-5.5] \quad (5)$$

The term multiplying F_{HW} accounts for epistemic uncertainty in hanging wall scaling. It is a maximum at sites on top of the hanging wall (R_{JB}=0) and decays to the footwall and neutral site epistemic uncertainty as R_{JB} increases (p_8 is negative). The coefficients of Eq. (5) are given in Excel file:

Hanford_GMC_Crustal_Median_Scaling_Coefficients.xlsx

The host-to-target scaling factors are independent of the oscillator period and the three values are indicated in Figure GMC1. The weights on all branches of the logic-tree for median ground motions from crustal earthquakes are also indicated in the figure.

Median Motions from Subduction Earthquakes

The preliminary GMC logic-tree for median spectral accelerations due to subduction earthquakes uses a new GMPE, adapted from the BCHydro GMPE as a backbone. The full logic tree has 72 branches, as can be inferred from Figure GMC2, below.

The backbone model is adjusted to the local site conditions (V_s profile), but this is done as the final step since the adjustment depends on the predicted median spectra for a specific scenario. No kappa correction is applied. For the backbone GMPE, branching is applied to model the epistemic uncertainty, with branches for different magnitudes at which the magnitude scaling changes (ΔC1), for uncertainty in the anelastic attenuation over large distances (θ_6), and for alternative median values. The branches for

alternative median values reflect the composite effect of uncertainty in the median and host-to-target adjustments.

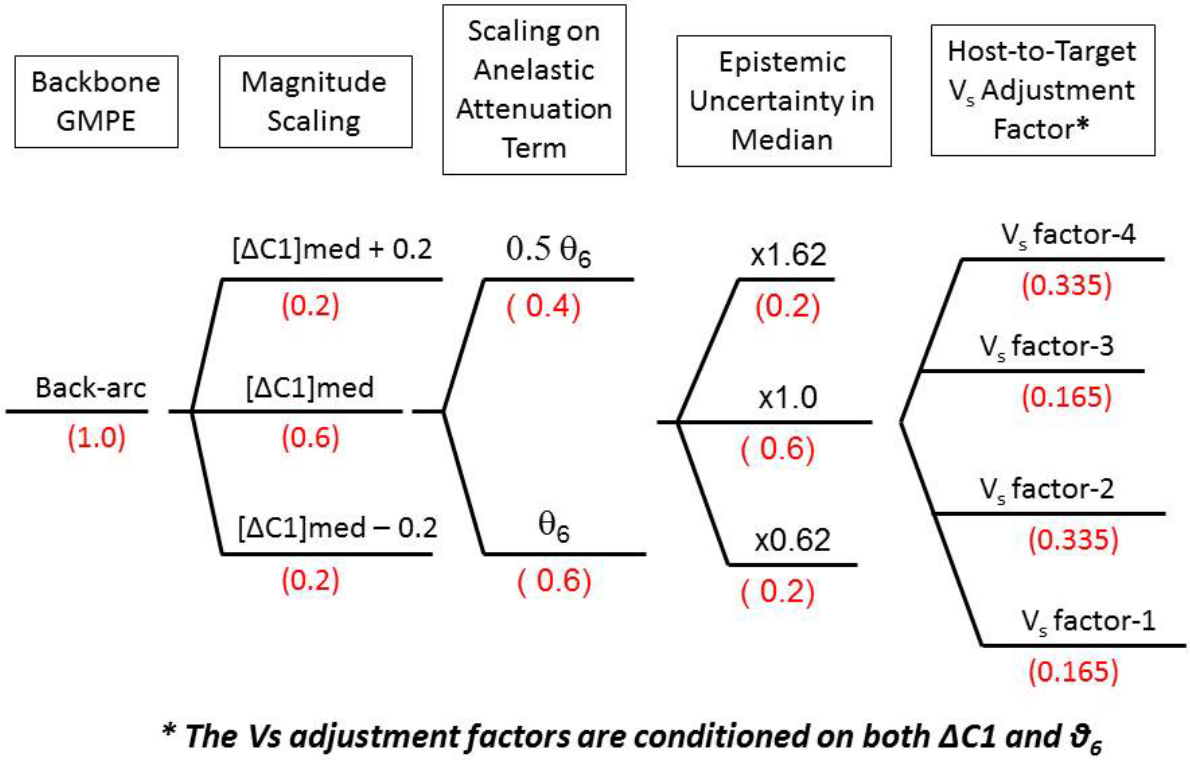

Figure GMC2. Logic-tree for median motions from subduction earthquakes.

The backbone equation for the prediction of spectral accelerations, *y* (in units of *g*), is given in Equation (6), and is modified from the original BCHydro model:

$$\ln(\boldsymbol{y}) = \boldsymbol{\theta}_1 + \boldsymbol{\theta}_4 \Delta \boldsymbol{C}_1 + (\boldsymbol{\theta}_2 + \boldsymbol{\theta}_{14} \boldsymbol{F}_{event} + \boldsymbol{\theta}_3 (\boldsymbol{M} - 7.8)) \ln(\boldsymbol{R} + \boldsymbol{C}_4 \boldsymbol{e}^{(\boldsymbol{M}-6)\boldsymbol{\theta}_9}) + \boldsymbol{\theta}_6 \boldsymbol{R} + \boldsymbol{\theta}_{10} \boldsymbol{F}_{event}$$
$$+ \boldsymbol{f}_{Mag}(\boldsymbol{M}) + \boldsymbol{f}_{depth}(\boldsymbol{Z}_h) + \boldsymbol{f}_{FABA}(\boldsymbol{R}) + \boldsymbol{f}_{site}(\boldsymbol{PGA}_{1000}, \boldsymbol{V}_{s30}) \qquad (6)$$

The model for magnitude scaling is:

$$\boldsymbol{f}_{Mag}(\boldsymbol{M}) = \boldsymbol{\theta}_4[\boldsymbol{M} - (\boldsymbol{C}_1 + \Delta \boldsymbol{C}_1)] + \boldsymbol{\theta}_{13}(10 - \boldsymbol{M})^2 \qquad \boldsymbol{M} \le \boldsymbol{C}_1 + \Delta \boldsymbol{C}_1 \qquad (7a)$$

$$\boldsymbol{f}_{Mag}(\boldsymbol{M}) = \boldsymbol{\theta}_5[\boldsymbol{M} - (\boldsymbol{C}_1 + \Delta \boldsymbol{C}_1)] + \boldsymbol{\theta}_{13}(10 - \boldsymbol{M})^2 \qquad \boldsymbol{M} > \boldsymbol{C}_1 + \Delta \boldsymbol{C}_1 \qquad (7b)$$

The model for depth scaling is:

$$f_{depth}(Z_h) = \theta_{11}(Z_h - 60)F_{event} \tag{8}$$

The model for forearc/backarc scaling is:

$$f_{FABA}(R) = \left[\theta_8 \ln\left(\frac{\max[R,40]}{40}\right)\right]F_{FABA} \qquad F_{event} = 1 \tag{9a}$$

$$f_{FABA}(R) = \left[\theta_{16} \ln\left(\frac{\max[R,40]}{40}\right)\right]F_{FABA} \qquad F_{event} = 0 \tag{9b}$$

where F_{FABA} is 0 for forearc (or unknown) and 1 for backarc sites.

The predictor variables in these equations are as follows:

M	Moment magnitude
$C_1 + \Delta C_1$	Magnitude at which magnitude scaling changes; (C_1 is always equal to 7.8)
Z_h	Focal depth (km)
F_{event}	0 for interface events, 1 for intraslab events
R	R_{RUP} for $F_{event} = 0$, R_{hyp} for $F_{event} = 1$
V_{s30}	A value of 760 m/s is used

The site-response scaling model, for sites with V_{s30} less than V_{lin} is:

$$f_{site}(PGA_{1000}, V_{s30}) = \theta_{12} \ln\left(\frac{V_s^*}{V_{lin}}\right) - b.\ln(PGA_{1000} + c) + b.\ln\left[PGA_{1000} + c\left(\frac{V_s^*}{V_{lin}}\right)^n\right] \tag{10a}$$

and for sites with $V_{s30} \geq V_{lin}$ is:

$$f_{site}(PGA_{1000}, V_{s30}) = \theta_{12} \ln\left(\frac{V_s^*}{V_{lin}}\right) + b.n.\ln\left(\frac{V_s^*}{V_{lin}}\right) \tag{10b}$$

The predictor variables in Eq.(10) are the following:

PGA_{1000}:	Median PGA for V_{s30} = 1,000 m/s
V_s^*:	1,000 m/s if V_{s30} > 1,000 m/s; V_{s30} for $V_{s30} \leq$ 1,000 m/s

The values of the coefficients of Equations (6) through (10) for the 20 response periods are given in Excel file ***Hanford_GMC_Subduction_Median_Coefficients.xlsx.***

The values of the V_s adjustment factors, which are specific to each combination of ΔC1 and θ_6 (hence there are six sets of values for each of the 5 hazard calculation sites) are listed in Excel file ***Hanford_GMC_Subduction_Vsfactors.xlsx*.**

Sigma Model for Crustal Earthquakes

The structure of the sigma logic-tree for crustal earthquakes consists of 2 branches representing different assumptions on the distribution shape, and 3 branches representing different values of the standard deviation (sigma), as illustrated in Figure GMC3 below.

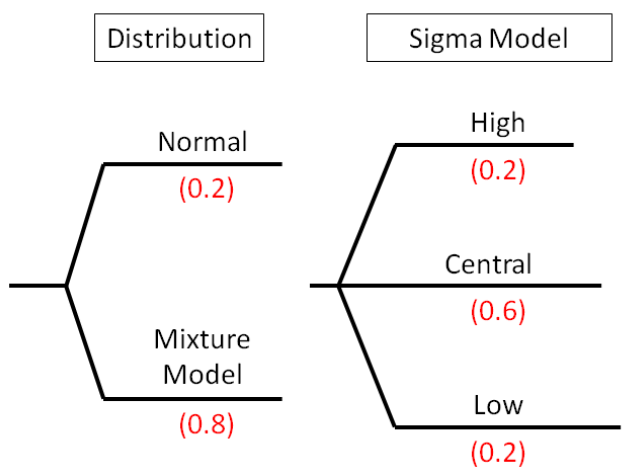

Figure GMC3. Logic-tree for sigmas associated with medians from crustal earthquakes.

Tables in Excel File ***Hanford_GMC_sigma_model.xlsx*** contain the values for sigma corresponding to the logic tree shown above. The values on tab "Crustal_Normal" contain the values for the model where the distribution is modelled as a single lognormal distribution. For the mixture model, the conditional probability of exceeding a specific ground motion value *z* is given by the equation:

$$P(Z > z) = w_{Mix1}\left\{1 - \Phi\frac{(z-\mu)}{\sigma_{Mix1}}\right\} + w_{Mix2}\left\{1 - \Phi\frac{(z-\mu)}{\sigma_{Mix2}}\right\} \qquad (11)$$

In Equation (11) w_{Mix1} and w_{Mix2} are the mixing proportions, which are both equal to 0.5. The values of σ_{Mix1} and σ_{Mix2} are listed on tabs “Crustal_Mixture_1” and “Crustal_Mixture_2”, respectively.

For the crustal model, the values of σ are magnitude dependent for both the normal and mixture models. The value of σ for any specific magnitude is computed from the relationship:

$$\sigma = \sigma_1 + \frac{\sigma_2 - \sigma_1}{2}[\min(\max(M, 5), 7) - 5] \tag{12}$$

where σ_1 and σ_2 are either the normal values or the mixture values.

Sigma Model for Subduction Earthquakes

The structure of the sigma logic-tree for subduction earthquakes is identical to that for crustal earthquakes. The only difference is that the values of σ are magnitude and period independent. The values of σ for the normal model are listed on tab “Subduction” in Excel File ***Hanford_GMC_sigmamodel.xlsx*** and the values for the mixture model are listed on tab “Subduction” in Excel File ***Hanford_GMC_sigmamodel.xlsx***. The mixture model is implemented using Equation (11).